

## Computational Study of Flow in a Micro-Sized Hydrocyclone

Guofeng Zhu\*, Jong-Leng Liow and Andrew Neely

School of Engineering and Information Technology  
UNSW@ADFA, Canberra, ACT 2600, Australia

### Abstract

We investigated the flow in a micro-hydrocyclone of 5 mm diameter. The micro-hydrocyclone will provide a novel approach to the separation of fine particle streams within a micro-device. The micro-hydrocyclone is a 1:15 scale of a 75 mm hydrocyclone. Whilst industrial hydrocyclones usually operate in the turbulent regime with an inlet Reynolds number of  $10^5$ - $10^6$ , the micro-hydrocyclone operates in the laminar regime with an inlet Reynolds number of the order of  $10^2$ . In contrast to the axisymmetric and well-developed tangential velocities profiles seen in the 75 mm hydrocyclone, the tangential velocities in the 5 mm micro-hydrocyclone were found to change and decay substantially from the inlet to the underflow due to viscous effects and a short residence time. The laminar flow does not reach a steady flow profile until an axial distance of  $z=12$  mm. The strong viscous dissipation damps out the recirculating flow observed in the large hydrocyclone and causes the locus of zero vertical velocity (LZVV) to terminate within the micro-hydrocyclone.

### Introduction

In recent years, the development of the micro-reactor has progressed significantly. However, micro-devices for separating out the products and wastes have yet to be developed. The lack of useful micro-devices for handling solids in the product streams has limited the application of micro-reactor technology to a wider range of industrial reactions [11]. The dearth of investigations is because the equipment for unit operations has extremely complex internals and moving parts make the miniaturization difficult.

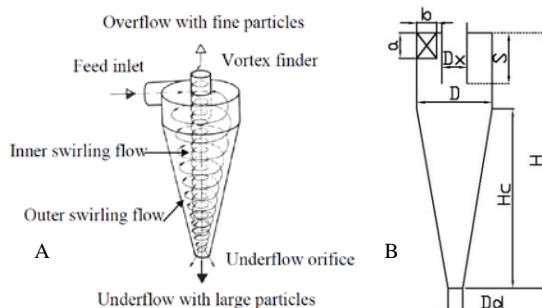


Figure 1. (A) A typical hydrocyclone configuration [12]. (B) Schematic of a hydrocyclone with the characteristic dimensions.

In the last 50 years, there has been a rapid growth in the application of hydrocyclones for particle separation in the chemical and mineral industries. A typical hydrocyclone (figure 1A) consists of a cylindrical body with a central tube (vortex finder) and a conical body with an underflow orifice. The fluid is injected tangentially through the feed inlet into the hydrocyclone causing the outer and inner swirling flows and generating centrifugal force within the device. This centrifugal force field brings about a rapid classification of particles based on particle size difference. Large particles are centrifuged outwards to the hydrocyclone wall and leave through the underflow orifice with

\*Corresponding author

the outer swirling flow. Fine particles dragged in by the fluid flow are removed by the inner swirling flow through the overflow in the vortex finder [5]. The particle size at which 50% separation efficiency to a hydrocyclone underflow occurs is defined as the cut size. As the majority of particles finer than the cut size will be collected from the overflow, a smaller cut size represents the ability to separate finer particles [12].

As similarity arguments have shown that the cut size is proportional to the square root of cyclone diameter [5], a hydrocyclone with a smaller diameter should be able to provide a smaller cut size to separate finer particles. The smallest hydrocyclone used in industry and research is 10 mm in diameter. Pasquier and Cilliers [8] used 10 mm hydrocyclones to dewater quartz slurry with a cut size around 3  $\mu\text{m}$ . However, the separation efficiency of fine particles in the 0.2 to 2  $\mu\text{m}$  range were found to increase as the particle size decreased. This phenomenon is known as the fishhook effect, the main cause of which is believed to be the entrainment of fine particles by large particles [7]. Cilliers and Harrison [4] reported the results on the dewatering of yeast (dominant cell diameter: 4.5–5.5  $\mu\text{m}$ ) in a 10 mm hydrocyclone. A high cell concentration ratio of 2.0 at a recovery of 30% could be achieved with the absence of cell breakage after a single separation. Pinto *et al.* [10] employed 10 mm hydrocyclones to separate Chinese hamster ovary cells (diameter: 8–40  $\mu\text{m}$ ) from exhausted medium. High recovery (>97%) and low cell viability losses (<15%) were achieved. Clearly, the current studies on small hydrocyclones do suggest that fine particle separation is achievable, but studies to investigate the parameters controlling small hydrocyclone operations, especially how fine particle separation is influenced by particle interaction, are lacking.

As smaller hydrocyclones hold the promise of separating finer particles, there is a need for research into miniaturised hydrocyclones with diameters less than 10 mm (defined as a micro-hydrocyclone in this paper) which are expected to provide a novel method for separating fine particle streams in a micro-device. While industrial hydrocyclones usually operate in the turbulent regime with the inlet Reynolds number of  $10^5$ - $10^6$ , the micro-hydrocyclone operates in the laminar/transitional regime with the inlet Reynolds number in the order of  $10^2$ - $10^3$  due its size and capacity.

A considerable amount of research has been performed using computational fluid dynamics (CFD) to model turbulent flows in hydrocyclones, but there are few computational studies of the laminar/transitional flow in micro-hydrocyclones. A pioneering work can be traced to Petty and Parks [9], in which the fluid flow in a 5 mm oil/water cylindrical shaped micro-hydrocyclone was modelled. However, the non-conventional cylindrical hydrocyclone in their study focused on liquid-liquid separation rather than particle separation, and the paper only provided the overall velocity contours without further exploring the characteristics of the fluid structure.

Hsieh [6] studied a 75 mm hydrocyclone, where an air-core was formed. He used laser-Doppler to measure the velocity profiles of the water flow in the hydrocyclone. Brennan [3] modelled the turbulent fluid flow of this hydrocyclone for an inlet velocity of 2.2 m/s with a Reynolds stress model (RSM), and the air-core was modelled with a volume of fluid (VOF) model with good agreement with Hsieh's experimental data.

In this paper, we studied the fluid flow in a micro-hydrocyclone with a diameter of 5 mm by CFD modelling. The micro-hydrocyclone is a 1:15 scale of the 75 mm hydrocyclone. We also reproduced Brennan's modelling results with the Reynolds stress model (RSM) and volume of fluid (VOF) model to obtain the turbulent fluid flow profile in the 75 mm hydrocyclone. Velocity profiles between the 75 mm hydrocyclone and 5 mm micro-hydrocyclone were compared to highlight the differences in flow behaviour.

### CFD Model

Fluid dynamics models for a micro-hydrocyclone have two main parts, the mass balance and momentum balance, which are described by the continuity equation and momentum equation respectively. As the flow is in the steady-state laminar regime, no turbulence model is required. Under steady-state conditions, the equations for mass and momentum balance for incompressible flow in a micro-hydrocyclone are as follows:

$$\nabla \cdot (\rho \vec{v}) = 0 \quad (1)$$

$$\nabla \cdot (\rho \vec{v} \vec{v}) = -\nabla p + \nabla \cdot (\vec{\tau}) + \rho \vec{g} \quad (2)$$

where  $\vec{v}$  is the velocity vector,  $\rho$  fluid density,  $p$  is the static pressure,  $\vec{\tau}$  is the stress tensor, and  $\vec{g}$  is the gravitational body force. The stress tensor is given by

$$\vec{\tau} = \mu(\nabla \vec{v} + \nabla \vec{v}^T) \quad (3)$$

where  $\mu$  is the molecular viscosity in this equation.

### Simulation Conditions

A schematic diagram of a hydrocyclone with characteristic dimensions is shown in figure 1B. The dimensions of the 5 mm micro-hydrocyclone and the original 75 mm hydrocyclone are shown in table 1. An unstructured mesh was used to grid the micro-hydrocyclone. Near the hydrocyclone wall and vortex finder wall, the mesh was refined to capture the sharp change in velocity in the boundary layers for the 75 mm case.

Geometrical properties	5 mm micro-cyclone (mm)	75 mm hydro-cyclone (mm)
Diameter, $D$	5	75
Total height, $H$	16.82	252
Conical section height, $H_c$	11.82	177
Overflow diameter, $D_x$	1.67	25
Vortex finder length, $S$	3.34	50
Feed inlet dimensions, $a \times b$	1.67 × 1.34	25 × 20
Underflow diameter, $D_d$	0.84	12.5

Table 1. Dimensional details of the hydrocyclones simulated

The CFD code FLUENT V12.0 was used to model the flow in double precision using. The pressure interpolation scheme used was PRESTO (pressure staggered option), which is well-suited for the steep pressure gradients involved in swirling flows. The SIMPLE algorithm was used for coupling the pressure and velocity. A third-order accurate QUICK scheme was used for spatial discretisation. A velocity inlet boundary condition was used at the hydrocyclone inlet, while the overflow and underflow outlets used the pressure outlet condition. The gauge pressure at the two outlets was set to 0 Pascal. The physical constants of the liquid phase were set as those of water at 20°C.

The convergence criteria used were that the mass flow rates of the overflow and underflow did not change with time, and the discrepancy of the global mass balance was below 0.5%. Mesh independence occurred at a mesh density of  $3 \times 10^6$  cells, and the results reported are from this simulation. In the micro-hydrocyclone, the swirling flow is not strong enough to generate a negative pressure central region to form an air core, thus the micro-hydrocyclone is fully filled with water. The average inlet velocity into the micro-hydrocyclone is 0.1 m/s. A fully developed velocity profile, obtained separately from the simulation of a long inlet pipe, was used as the inlet boundary condition.

## Results and Discussion

### Formation of the Steady Flow Profile

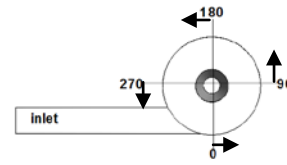


Figure 2. Definitions of the angles and direction of the positive tangential velocity

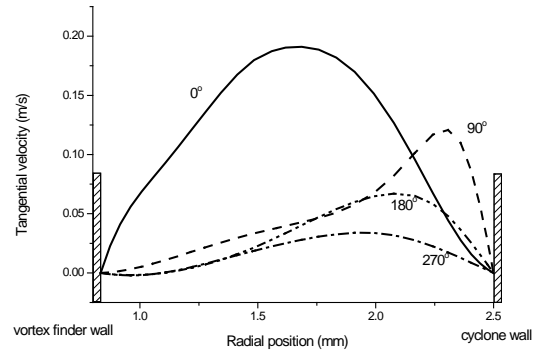


Figure 3. Tangential velocities for the 5 mm micro-hydrocyclone at  $z=0.83$  mm in four equally spaced locations.

Figure 2 shows a schematic for the definitions of angles and direction of positive tangential velocity in a hydrocyclone. The axial distance,  $z$ , is measured as positive in the downward direction from the top of the cyclone. Figure 3 shows the tangential velocity at an axial distance of  $z=0.83$  mm (equivalent to half of the inlet height) for the micro-hydrocyclone at four equally spaced locations around a circular plane. At  $0^\circ$ , the fully developed parabolic velocity profile of the inlet condition can be seen. Between  $0^\circ$  to  $90^\circ$ , the linear momentum progressively transfers to angular momentum due to the curvature of the wall resulting in the maximum velocity shifting from the centre towards the cyclone wall. The inlet flow creates a high-pressure region as it approaches the curved wall and as the fluid is incompressible, the flow is forced to change direction forcing the fluid to rotate and move axially down the cyclone. From  $90^\circ$  to  $270^\circ$ , as the rotating flow profile develops, the maximum tangential velocity moves away from the outer wall due to momentum transfer and decreases in magnitude as the fluid progressively diverts to the downward axial direction to satisfy continuity.

Figure 4 shows the tangential velocities for the micro-hydrocyclone in the  $0^\circ$ – $180^\circ$  plane just below the position of the vortex finder. From  $z=4$  to 10 mm (figure 4A), the laminar flow profile develops quickly and changes markedly. Figure 4B shows that the laminar swirling flow reaches a steady flow profile at approximately  $z=12$  mm and below. Thereafter the flow profiles are more symmetric and the position of the velocity maximum

can be seen to be positioned at the same dimensionless distance ( $r^*$ ) ( $r^* = r_{v=\max}/r$ , where  $r_{v=\max}$  is the radius at the maximum tangential velocity and  $r$  is the radius of the corresponding location at each  $z$ ). In contrast, the turbulent wall boundary layers in the 75 mm hydrocyclone is thin and have an identical profile (figure 5), which agrees with the analytical finding by Bloor and Ingham [2] that the turbulent boundary layer thickness is approximately the same throughout the cyclone body.

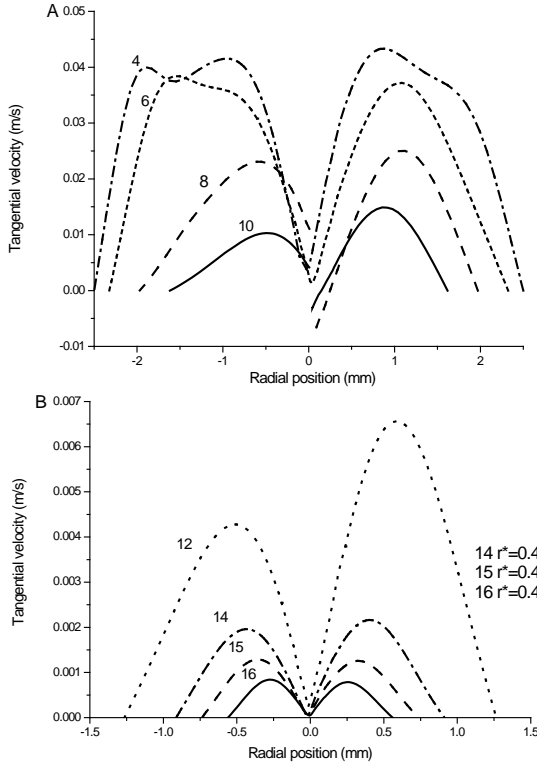


Figure 4. Tangential velocities for the 5 mm micro-hydrocyclone in the  $0^\circ$ – $180^\circ$  plane at: (A)  $z=4, 6, 8$  and  $10$  mm. (B)  $z=12, 14, 15,$  and  $16$  mm.

**Tangential Velocities**

Figure 5 also shows the typical tangential velocity profile observed in large hydrocyclones, where the envelopes of constant tangential velocity are coaxial cylinders and the tangential velocity is axisymmetrically distributed. The free vortex flow is evident in the outer region. In contrast, figures 4A & B show the rapid decay of the tangential velocity in the micro-hydrocyclone from the inlet to the underflow, and the velocity distribution is asymmetric. A negative tangential velocity region is found at  $z=6$  and  $8$  mm where the vortex centre is not aligned with the central axis. The asymmetry could be due to the shorter residence time in the micro-hydrocyclone and that the flow field is laminar in nature but a more detail study is required to elucidate its impact on the micro-hydrocyclone performance.

The inlet Reynolds number for large hydrocyclones is of the order of  $10^5$  to  $10^6$ , resulting in a highly turbulent flow where inertial effects dominate in the cyclone body, except for the regions close to the cyclone wall and central axis. Therefore, the swirling flow inside can be considered to be inviscid flow for which the angular momentum is conserved. The tangential velocities display a free vortex flow pattern and remain constant from the inlet to underflow. In contrast, the inlet Reynolds number for the micro-hydrocyclone is of the order of  $10^2$ , resulting in a laminar flow where the viscous effects are important. Consequently, the velocity decreases markedly from the inlet to underflow orifice. In the view of fluid residence time, the average residence time in the micro-hydrocyclone (of the order of 1.5-2 revolutions) is considerably shorter than that in the

hydrocyclone (more than 20 revolutions). The longer residence time allows the axisymmetric flow to be built in large hydrocyclones, whereas the short residence time results in the asymmetric flow the micro-hydrocyclone.

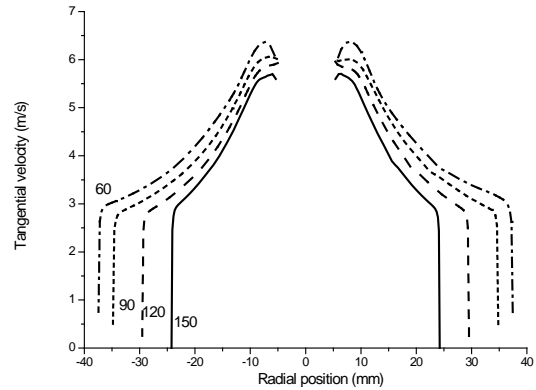


Figure 5. Tangential velocities for the 75 mm hydrocyclone at equivalent locations to figure 4A at distances  $z=60, 90, 120$  and  $150$  mm in the  $0^\circ$ – $180^\circ$  plane with plots offset by a fixed height of  $0.25$  m/s to avoid overlapping of the curves. The central region contains an air core.

**Axial Velocities**

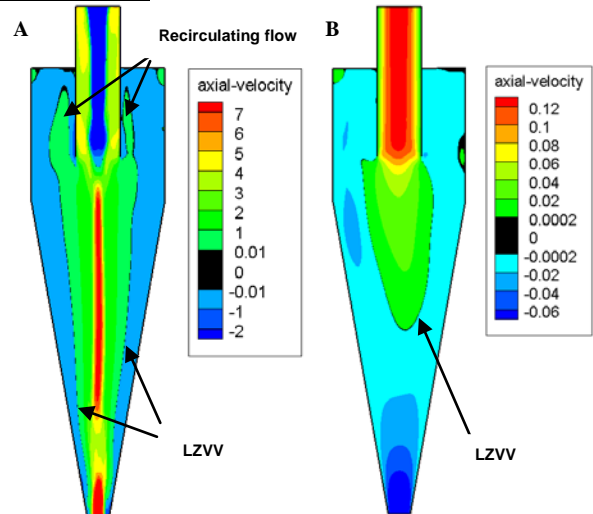


Figure 6. Comparison of the axial velocity distributions (m/s, upward is positive and downward is negative) in the 75 mm hydrocyclone (A) and 5 mm micro-hydrocyclone (B).

Figure 6 shows the axial velocity distributions for the 75 mm hydrocyclone and 5 mm micro-hydrocyclone in the  $0^\circ$ – $180^\circ$  plane. For the 75 mm hydrocyclone, a clockwise recirculating flow exists in the region between the vortex finder outer wall and cyclone wall where the fluid moves up vortex finder wall and down the cyclone wall. This is caused by the large upward flow that cannot be completely removed through the vortex finder resulting in flow part the vortex finder. In contrast, the micro-hydrocyclone does not have a recirculating flow as the fraction of fluid exiting through the vortex finder is smaller. Fine particle retention by the recirculating flow leads to these particles being transferred to the underflow; hence an absence of the recirculating flow may improve the fraction of fine particles exiting at the overflow.

Below the vortex finder, the locus of zero axial or vertical velocity (LZVV), which locates the division between upward and downward swirling flows, can be found in both hydrocyclones (black dash curves in figure 6). In the region between the cyclone wall and the LZVV, the fluid flows downwards to the underflow, while in the region inside the LZVV, the fluid flows upwards. The LZVV locates as a conical envelope extending to the underflow orifice in the 75 mm hydrocyclone. According to the

analytical study by Bloor and Ingham [1], the ratio of the LVZZ conical angle to the cyclone geometrical conical angle is 0.6 for industrial hydrocyclones which is evident for the 75 mm hydrocyclone. In contrast, the LZVV for the micro-hydrocyclone locates with a parabolic shape and terminates at an axial distance of around two-thirds of the total cyclone height. Consequently, the downward swirling flow region is larger resulting in a larger fraction of the feed exiting through the underflow orifice. The reduction of the overflow in the micro-hydrocyclone may result in higher separation efficiency of large particles to the underflow.

### Radial Velocities

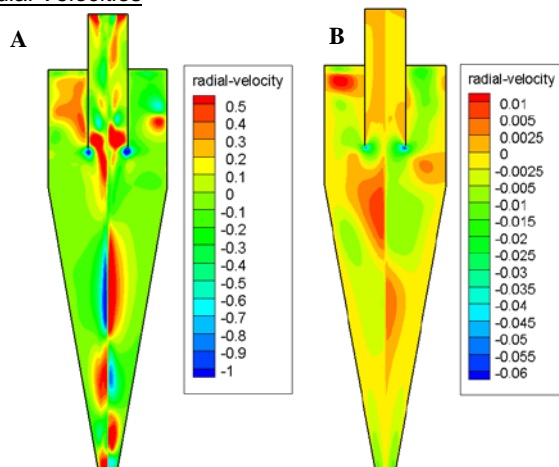


Figure 7. The distribution of radial velocities (m/s, outward is positive and inward is negative) in the 75 mm hydrocyclone (A) and 5 mm micro-hydrocyclone (B).

The radial velocities are orders of magnitude smaller than the tangential and axial velocities. It is similar in order of magnitude to the fluctuating velocities for the 75 mm hydrocyclone. Hence, radial velocities could not be measured directly and Hsieh [6] estimated the radial velocities by satisfying continuity using the measured tangential and axial velocities with the assumption that the flow is axisymmetric. He found that the direction of the radial velocities was inward pointing towards the central axis below the vortex finder. Based on the assumption of the axisymmetric flow, the analytical results of Bloor and Ingham [1] confirmed that the radial velocities below the vortex finder were directed inwards. The radial velocity distribution calculated by the CFD model shows both inward and outward directed velocities (figure 7). Below the vortex finder, the radial velocities are inward pointing in the outer region, whereas for the region along the central axis, the radial velocities alternated in direction down the axis for both in the 75 mm hydrocyclone and the 5 mm micro-hydrocyclone. The alternation is due to the asymmetric vortex flow inside the hydrocyclones. Although the flow can be regarded as symmetric in the large hydrocyclone, the solution is affected by small discrepancies in velocities. Moreover, the vortex centre is not precisely located along the central axis at each axial location. Consequently, some radial flows occur where the fluid crosses from one side to the other along the central axis. For the micro-hydrocyclone, the asymmetry of the radial velocities is more severe. Apart from the asymmetry of the vortex, high inward radial velocities, located immediately below the vortex finder wall, exists in both of the hydrocyclones. The radial velocities there results from the strong downward flow from the outer wall of the vortex finder that reverses its direction over a short distance. This result in the short circuiting of unclassified large particle from the vortex finder outer wall to the overflow, which reduces the hydrocyclone separation performance.

### Conclusions

In this paper, a CFD model was used to investigate the flow in a micro-hydrocyclone with a diameter of 5 mm. The micro-hydrocyclone is a 1:15 scale of a 75 mm hydrocyclone. While industrial hydrocyclones usually operate in the turbulent regime with the inlet Reynolds number of  $10^5$ - $10^6$ , the micro-hydrocyclone operates in the laminar regime with the inlet Reynolds number of the order of  $10^2$ .

The tangential velocities for the 75 mm hydrocyclone display a free vortex flow pattern and remain constant from the inlet to underflow. In contrast, the inlet Reynolds number for the micro-hydrocyclone is of the order of  $10^2$ , resulting in a laminar flow where the viscous effects are important. Consequently, the velocity decreases markedly from the inlet to underflow orifice. This rapid change in velocity is exacerbated by the small average residence time in the micro-hydrocyclone (of the order of 1.5–2 revolutions) being considerably shorter than that in the hydrocyclone (more than 20 revolutions). For the micro-hydrocyclone, a steady flow profile is reached only after an axial distance of  $z > 12$  mm whereas it is established much earlier in the 75 mm hydrocyclone. The locus of zero vertical velocity (LZVV) in the micro-hydrocyclone occupied a much smaller region centred in a parabolic shape around the vortex finder inlet while in the 75mm hydrocyclone the LZVV extends into the underflow outlet.

Further work is required to quantify the efficiency of the micro-hydrocyclone in separating fines and this will be the focus of future work.

### Acknowledgments

Guofeng Z acknowledges the financial support of the China Scholarship Council.

### References

- [1] Bloor, M. & Ingham, D., Theoretical investigation of the flow in a conical hydrocyclone, *Chem. Eng. Res. Des.*, **51**, 1973, 36-41.
- [2] Bloor, M. & Ingham, D., Boundary layer flows on the side walls of conical cyclones, *Chem. Eng. Res. Des.*, **54**, 1976, 276-280.
- [3] Brennan, M., CFD simulations of hydrocyclones with an air core - Comparison between large eddy simulations and a second moment closure, *Chem. Eng. Res. Des.*, **84**, 2006, 495-505.
- [4] Cilliers, J.J. & Harrison, S.T.L., The application of mini-hydrocyclones in the concentration of yeast suspensions, *Chem. Eng. J.*, **65**, 1997, 21-26.
- [5] Hoffmann, A. & Stein, L., *Gas Cyclones and Swirl Tubes: Principles, Design, and Operation*, Springer Verlag, 2007.
- [6] Hsieh, K.-T., *Phenomenological model of the hydrocyclone*, The University of Utah, 1988.
- [7] Neesse, T., Dueck, J., & Minkov, L., Separation of finest particles in hydrocyclones, *Miner. Eng.*, **17**, 2004, 689-696.
- [8] Pasquier, S. & Cilliers, J.J., Sub-micron particle dewatering using hydrocyclones, *Chem. Eng. J.*, **80**, 2000, 283-288.
- [9] Petty, C. & Parks, S., Flow structures within miniature hydrocyclones, *Miner. Eng.*, **17**, 2004, 615-624.
- [10] Pinto, R.C.V., Medronho, R.A., & Castilho, L.R., Separation of CHO cells using hydrocyclones, *Cytotechnology*, **56**, 2008, 57-67.
- [11] Roberge, D., *et al.*, Microreactor technology: A revolution for the fine chemical and pharmaceutical industries?, *Chem. Eng. Technol.*, **28**, 2005, 318-323.
- [12] Svarovsky, L., *Hydrocyclones*, Holt, Rinehart and Winson, 1984.